

Electrical conductivity particle detector for use in biological and chemical micro-analysis systems

Bruce K. Gale^a, Karin D. Caldwell^{a,c}, A. Bruno Frazier^{a,b}

Departments of ^aBioengineering, ^bElectrical Engineering, and ^cChemistry
University of Utah, Salt Lake City, UT 84112

ABSTRACT

This work introduces an integrated electrical detector for use as a conductivity or impedance based detection system for miniaturized biochemical analysis systems such as liquid chromatography or field flow-fractionation systems. Motivation for use of an on-chip conductivity detector is given. The design, fabrication, and characterization of the detector in the conductivity-based detection mode are described. Critical parameters of the conductivity detector, such as time constants, detection limits, and the effects of flow rate and applied voltage on detector response, are measured. In addition, the on-chip detector is compared to a conventional off-chip, UV-based detection system.

The conductivity detector was fabricated by creating low impedance electrodes on the top and bottom surface at the end of a typical separation channel. The detector was shown to easily detect particles in the working concentration range of a typical separation system at low applied voltages. The measured time constants averaged approximately 2 seconds and changed slightly with flow rate through the detector. This time constant is acceptable for typical separations that take minutes to complete. The detector was also shown to dramatically improve resolution and reduce peak broadening for the system when compared to an off-chip detector.

Keywords: Micromachining, conductivity detector, chromatography, field- flow fractionation

1. INTRODUCTION

Many of the recent medical and drug advances can be tied directly to improvements in chemical and biological analysis systems. These analysis systems are used to study all kinds of chemicals and biological molecules and to screen these particles for efficacy in various medical applications. These techniques include electrophoresis, gas and liquid chromatography, the various biosensor devices that use proteins, DNA, antibodies, cells, and other biological particulates (such as PCR). Of critical importance to all of these techniques is the detection, monitoring, and transduction methods used to collect, observe, and interpret the signals, separation, or reaction generated by the device. Almost every method for energy transduction has been used to measure and observe signals in these various devices including optical, electrical, mechanical, thermal, chemical, magnetic, and others. The most sensitive techniques and those generally used for the various analysis systems, and more specifically, chromatography systems are optical measurements involving either fluorescence or UV absorption and reflection.

The optical techniques generally used with chromatography systems have several disadvantages. They are generally very bulky, expensive, complex, and often require modification of the sample being detected in order to perform measurements. They are also very sensitive to physical movement and require considerable maintenance. While the UV extinction and light scattering techniques are quite robust and allow for a wide variety of sample types, they are also expensive and bulky. For large-scale labs with fixed laboratory equipment, these detection techniques provide high sensitivity and are well characterized and developed, but for use with portable equipment, and especially for use with the new crop of microscale analysis systems, more compatible, low-cost detection methods will need to be developed and tested.

Further author information-

B.K.G. (correspondence): Email: Bruce.Gale@m.cc.utah.edu; Telephone: 801-581-8611

K.D.C.: Email: Karin.Caldwell@m.cc.utah.edu

A.B.F.: Email: frazier@ee.utah.edu; Telephone: 801-585-7997

In recent years, a push has been made toward integrating a collection of microscale chemical and biological analysis systems on one chip- the so-called lab-on-a-chip design. While no one at yet has demonstrated a wide range of systems on one chip, a large number of individual biological and chemical analysis techniques have been demonstrated in a micro-scale system and have been implemented using micromachining technology. These systems include electrophoresis^{1,2,3,4,5,6,7,8}, free-flow electrophoresis^{9,10}, electrical field-flow fractionation (EFFF)^{11,12}, polymerase chain reaction (PCR)^{13,14,15,16}, gas chromatography^{17,18,19,20,21}, liquid chromatography^{22,23}, and hybrid systems^{24,25}. For a practical total analysis system, the systems must integrate sample handling, data processing, and data acquisition. Unfortunately, most current micromachined systems still rely on off-chip components to perform the bulk of the detection and signal processing duties, whether or not the actual detection takes place on or off chip. These detection systems are generally the same ones used for the corresponding macro-analysis system with slight modifications for working on the smaller microscale systems. In many cases, after processing the sample using the microscale device, the sample is moved off chip for analysis. Moving the sample off-chip, though, can be very detrimental in terms of resolution for chromatography systems²⁶, and measurement quality for other systems. The relatively large size of most detectors also limits the possibilities for parallel channel processing. Again, there is a great need for a simple on-chip detector for use with these micromachined analysis systems.

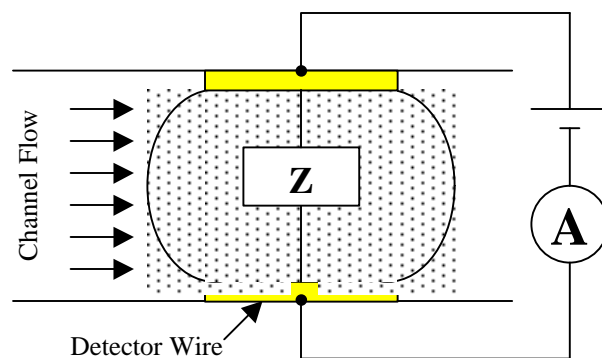


Figure 1. Schematic of electrical configuration of detector showing detection zone, flow in the channel, and unknown impedance in channel.

Several groups have proposed designs for detectors compatible with microscale devices and it is conceivable that several of the contemporary detection techniques could be miniaturized for integration with the micro-analysis systems. Micromachining is very compatible with VLSI and other semiconductor optical techniques, so we may very well see laser detectors on chip soon if they are not already in existence. Conversely, the trend in microscale analysis systems is away from silicon and towards glass and plastics which are less expensive, so many of the current detectors which rely on the semiconductor properties of silicon will not be applicable to the rising generation of devices. Thus there remains a need for a simple, micromachinable, inexpensive and robust detection system with application to a variety of devices and manufacturable on a number of different surfaces.

To solve this problem we propose a low-power detector capable of being used as a conductivity detector or an impedance spectroscopy based detection system²⁷. The work presented in this paper is focused on characterization of the detector for use as a conductivity-based detector. The detector consists of two parallel wires, a power source and a current meter (or impedance analyzer) for data collection and analysis. A small voltage is applied across the two wires and the current is measured between the wires. The sample is moved between the wires and any change in material between the wires will generally create a change in the measured current through the circuit. A schematic of this circuit is shown in Figure 1. The detector was fabricated specifically for detection of particles in an electrical field- flow fractionation systems, but has application to all field- flow fractionation devices as well as other chromatography and measurement systems.

2. THEORY

The theory behind the operation of this device is on the surface very simple, but after just slight analysis, the theory that governs this device becomes extremely complex and varies with the type of samples being used. To simplify our initial analysis and to demonstrate the efficacy of this device without going beyond the scope of this work, more complex theoretical analysis will be done in later communications and only the basic theory will be covered here.

The design for the device operates under the assumption that the sample of interest being detected or measured has impedance at least slightly different from that of the buffer carrying the sample. Thus, with a constant voltage applied across the detection zone, any change in the composition of the material between the electrodes will result in a change in the current through the circuit. This change in current can be measured in two ways: either by measuring the current directly using a current meter or by converting the current to some other easily measured signal. The current in most cases will be carried by ions in the buffer and will therefore result in redox reactions at the electrodes that comprise the detector.

The impedance of the buffer can be changed in several different ways that are dependent of the parameters for operation of the system as well as the sample being detected. The first way that a sample might change the impedance in the detection chamber is by being electrically conductive itself. In this case the sample reduces the impedance in the detection area by carrying additional current itself. The opposite effect makes up the second way in which the impedance might change. If impedance of the sample is higher than that for the bulk solution then the effective impedance seen by the detector increases, thus making current conduction more difficult. A third way in which the impedance may change is by interference with the double layer of ions that build up at the electrode surface.

The ionic double layer is caused by the constant potential applied to electrodes in solution. At the interface between the electrode and the solution, ions of opposite polarity collect near the surface of the electrode and oppose the imposed voltage created at the electrodes. Thus, a positively charged electrode will have a cloud of negative ions surrounding it while the oppositely charged electrode would be surrounded by positive ions. In effect the electrodes form a capacitor whose internal electric field is directly opposed by the electric field established by the surrounding ion clouds. It is important to note that the “thickness” of the double layer is highly dependent on the ionic strength of the buffer and is much greater for solutions with high ionic strength. The thickness of the double layer also depends on the velocity of the fluid and drops as the velocity increases²⁸. The net electric field between the electrodes at steady state is about 1 % of the applied field for DI water²⁹. The effect of the double layer is to reduce the current in the circuit substantially. In the event that the double layer is disturbed, either by dilution or being swept away, the current would be expected to rise in relation to the disturbance and then fall again as the disturbance is eliminated and steady state is reestablished. Thus, there are three general ways in which the impedance in the detection area might change and allow a sample to be detected. In most cases, we expect that a combination of these modes will determine the actual change in impedance.

Since the double layer is expected to play a significant role in the operation of this detector, an understanding of how the double layer affects the operation of the device is critical. The establishment of a double layer can be modeled as a first order system with a time constant, τ . This time constant is most easily seen when a step in voltage is applied to the system. There is an immediate jump in current to some nominal value predicted using Ohm’s law followed by an exponential decay in current to some steady state value dependent on the double layer thickness. Thus, assuming that a disturbance in the double layer occurs when most samples enter the detection area, the reestablishment of steady state will impact how quickly the detector can follow a “falling” signal. It should be noted here that the time constant as defined here for the detector is somewhat different from that generally used in instrumentation which measures how quickly the detector responds to changes in the input signal. Since the input here is generally a change in concentration of one analyte or another, it is extremely difficult if not impossible to know the input signal with any accuracy due to diffusion, convection, and other mixing agents and so it is extremely difficult to measure the time constant of the detector as it is normally defined. Since the time required for the instrument to follow a change in impedance is so small as to be insignificant, and any disturbance in the double layer can be considered to happen relatively quickly if not instantaneously, the only effect with potential to corrupt the measurement of the signal in the detector itself is the reestablishment of the double layer. Thus the time required for reestablishment of steady state can be considered the limiting factor in terms of bandwidth for the impedance detector.

Once it is known that a change in impedance will occur, the next question becomes what the magnitude of the change will be for a given sample and how does the signal relate to the concentration of that sample. In the simplest case, the response should relate directly to the concentration of the injected species. This would be the case for samples such as salt solutions that can be modeled as ideal particles with no mass or size. Only their charge and current carrying capacity would matter. For large particles where mass and size cannot be neglected, the component of current due to a particles ability to carry current would rise linearly, while size and mass would work together to create a nonlinear effect. For example, if we assume that we are attempting to detect spherical particles and the entire sample has a constant mass, the impedance and particle diameter would be related as given in equation 1 where R is the resistance and d the diameter of the particles. The inverse relationship is due to the fact that as the diameter of the particles increases the profile of the particles in the plane that opposes current conduction decreases. Thus, the detected signal would be expected to increase for smaller particle sizes which is not the case with many detectors.

$$R \propto \frac{1}{d} \quad (1)$$

Equation 1 indicates that for spherical particles the response is not directly related to concentration, but is rather a function of diameter. Thus, the concentrations of particles can be calculated only if the diameter of the particles is known. For small

particles, though, one would expect that concentration could be measured directly from the response of the detector. This simple view is limited by the presence of the double layer and the impact of the sample on the distribution of the double layer is not easily calculated, so many of the double layer effects will likely need to be established empirically if accurate concentration measurements are to be obtained. Fortunately, for many applications, only detecting the presence of a sample is required or else finding the center of a separation peak, both of which should be easily accomplished using the proposed impedance detector.

One potential problem associated with this detector in aqueous solutions is the electrolysis of water into hydrogen and oxygen. While the hydrogen and oxygen themselves do not cause a problem, the bubbles formed tend to increase noise in the detector and it has been demonstrated that a large jump in current occurs at the point that electrolysis begins. Since the current change due to samples moving through the detector is expected to be in the nanoampere range, a large baseline current may make it difficult if not impossible to measure any signal on top of a large baseline current potentially in the microampere range. Thus, electrolysis must be avoided.

One other area of interest is the detection volume that will be probed by the proposed detector. The current path is not limited to the area immediately between the electrodes, but fans out some distance into the channel in either direction. A finite element model of this effect is shown in Figure 2. Note the variation in current density across the channel indicating that particles traveling through will be affected differently. Thus, the response of the detector will also likely vary depending on the location of the detected particles, i.e. particles in the center of the channel may generate a slightly different signal than those closer to one of the electrodes.

Of critical importance in chromatography systems is resolution and peak broadening. Resolution is a measure how well a separation has been performed and peak broadening is a measure of how much a sample peak widens during its traversal of the separation channel. The detector used in the chromatography system can play a critical role in determining the amount of peak broadening that takes place. Mixing in the separation channel, which typically occurs in bends, expansions and contractions, or sharp geometries, is the usual cause for peak broadening. Structures of this type must be avoided, and the easiest way to do so is by placing the detector on chip. Peak broadening is typically measured in terms of plate heights: a term related to the length of a channel required to perform an incremental amount of separation. The lower the plate height, the more powerful the instrument. More information on peak broadening, plate heights, and resolution is available in chromatography texts and several of the references at the end of this paper.^{12,30}

3. FABRICATION

The detector was fabricated in channels specifically designed for field- flow fractionation, but with general applications as mentioned previously. The channel fabrication has been reported previously in connection with a micromachined electrical field- flow fractionation system.¹² One of the main advantages of this detector is its simple design. On its own it would only take 1 or 2 masks depending on the design, and

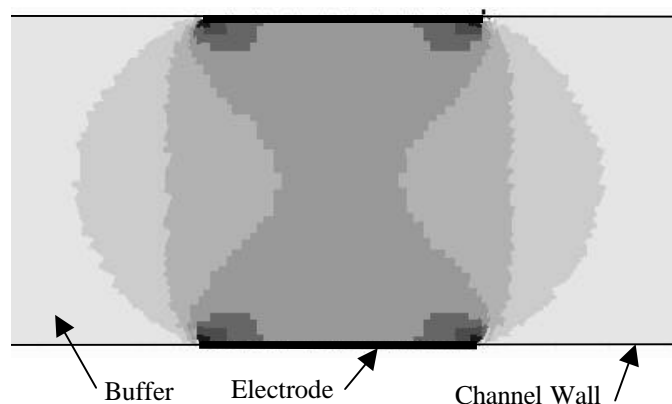


Figure 2. Finite element model of detector showing current density between the detector wires. Darker shading indicates higher current density. Notice the non-uniformity of the current and the expansion of the detection region out into the channel.

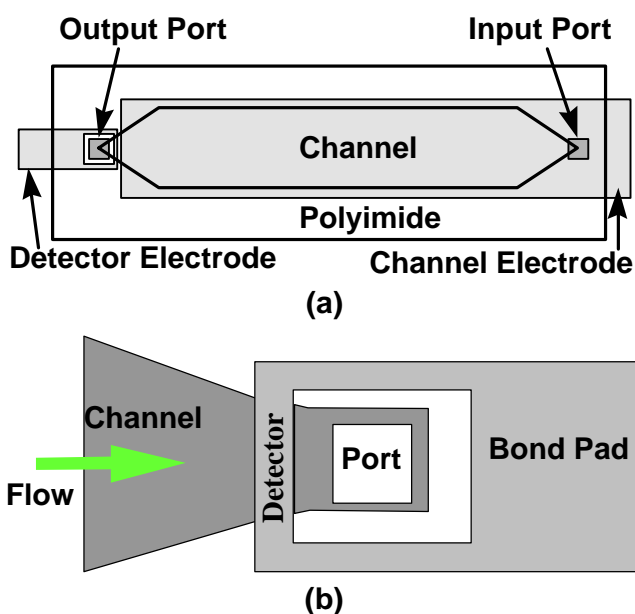


Figure 3. Schematic of detector. (a) Overview of channel and detector (b) Close up of detector.

was easily incorporated directly into the masks for the electrical field- flow fractionation system so no additional masks were required. The channel consists of two parallel plates with a spacing of 20-30 μm . The detector is fabricated by depositing 500 \AA of titanium followed by 2500 \AA of gold onto both plates that form the channel and then using photoresist to pattern the wires. The wire on the top plate is 100 μm in width while the wire on the other plate is 5, 25 or 100 μm in width. The layout of the detector is given in Figure 3. The width of the top wire is kept at 100 μm to facilitate alignment of the wires since alignment is generally done by hand under a microscope. For the purposes of this paper, all tests were done using a 25 μm wire. Once the channels were assembled, leads were attached to the bond pads using a conductive adhesive to allow a good electrical connection.

4. EXPERIMENTAL

The channel used for these experiments was 6 mm in width with a height of 26 μm . The ends of the channel tapered to entrance and exit ports at a 60° angle. Once the channel and detector were fabricated, they were connected to an HP 6128C DC Power Supply and an HP 3458A multimeter. The multimeter was connected to a PC for data collection and analysis using LabView. Connections, sample injection, pumps, and other hardware are identical to those used with micromachined field- flow fractionation systems.¹² DI water was the buffer used for all experiments.

The experimental matrix took into account the variation of three basic parameters: buffer flow rate, applied voltage and corresponding current, and sample size and composition. Flow rates through the detector were varied from 0.1–2.0 mL/hr (0.017-0.33 cm/s) which is the typical range for most separations that might use this detector. Voltages applied to the detector electrodes ranged between 2 and 8 V. For most detector characterization experiments the sample was acetone and was varied in concentration from 0 % to 100 %. The time constant, τ , defined earlier was also measured for a series of flow rates and voltages for comparison.

To perform the plate height measurements, 100 nL samples of acetone were injected into the system using both the on-chip detector described in this paper and an off-chip Linear UV detector for a series of flow rates. The width of the peaks were measured as well as the time required for the peak to elute. The plate height calculations were then performed using standard chromatography methods.³⁰

5. RESULTS

A micrograph of one side of the finished detector is shown in Figure 4. The actual width of the completed wire is 19 μm as compared to the nominal 25 μm . The slight

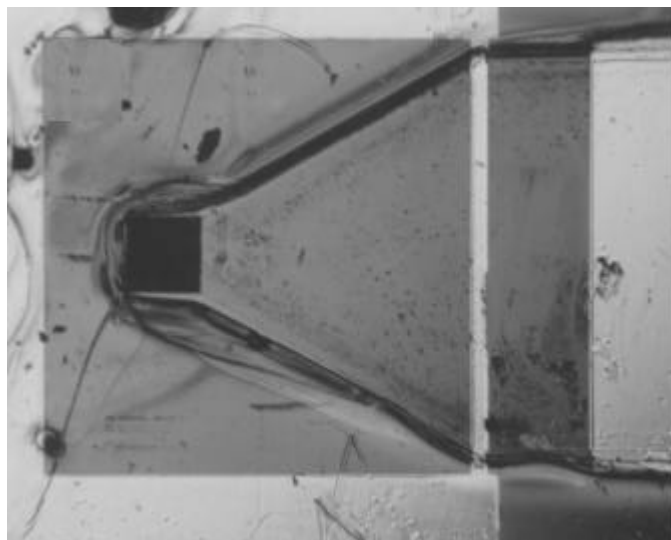


Figure 4. Photograph of fabricated detector showing a 19 μm detection wire across the channel and connections to the bond pad. The channel is defined using polyimide.

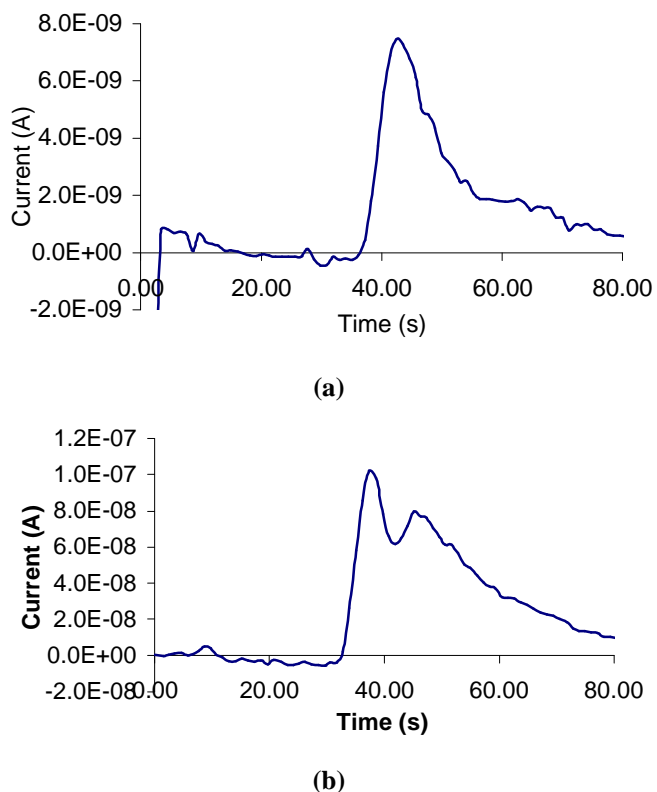


Figure 5. Typical peaks measured using impedance detector. (a) Shows a typical injection peak and some of the tailing that may be due to the slow response of the detector. (b) Sample showing a double injection which is an artifact of the injection process. Clearly the response time is fast enough to detect two closely spaced peaks.

reduction in wire width is due to overetching of the metals during fabrication.

Initial results from the detector were promising. The detector was clearly able to detect a number of different samples. A typical acetone peak is shown in Figure 5a. Note the very fast initial response to the peak and the slower drop off on the backside of the peak. While this behavior is somewhat typical for acetone peaks in other detectors and is likely due a high flow rate in the channel, the tailing is somewhat exaggerated and likely somewhat greater than reality due to the somewhat slower response of the detector in returning to a steady state current. The detector was fast enough though to detect a slight double injection, Figure 5b that was reported earlier during testing of a micromachined electrical field-flow fractionation system²⁶ and had completely escaped notice in an off-chip UV detector. Through use of the detector we were able to refine the injection process and eliminate the double peaks.

Figure 6 shows a graph of time constant data at a series of flow rates and voltages. The buffer was DI water and 0.1 μ L acetone samples were the input signal. This figure provides several items to note. First, the time constants to reach steady state were higher for the system at 3 V than at 4 V. This indicates that it takes longer to reach steady state at 3 V. The simple explanation may be that the lower voltage does not imbue the ions with a velocity as high as that when 4 V is applied and so it takes longer to equilibrate. On the flip side, one would expect that the double layer would be thicker at 4 V and require more time to set up. Further observation indicates that at lower voltages the time constant becomes less once again, though significant data is not presented here. The explanation may then be that there are a limited number ions available to establish the double layer and that at lower voltages the lower double layer thickness allows a smaller time constant while at higher voltages all of the ions available are used to form the double layer so the time constant depends on particle velocity only, which is a direct function of voltage. Thus the area of 3 V may be this maximum point indicating that the time constant is unlikely to go above 4 seconds and will be more generally in the range of 2 seconds.

Figure 6 also indicates a similar phenomenon occurs as flow rate increases. At low flow rates the time constant is relatively low and slowly increases with flow rate before falling off again. Our hypothesis is that at low flow rates there is little mixing or disruption as the double layer forms allowing it to form quickly. At high flow rates the shearing forces from the flow keep the double layer from ever reaching its maximum height and therefore steady state is reached earlier. In the middle of this range, at about 1 mL/hr, the shearing forces are not high enough to limit the growth of the double layer while at the same time significant enough to disrupt the growth of the double layer such that the time constant at this flow rate is higher than that for the surrounding flow rates.

Overall, the time constant data helps us better understand the mechanisms that are at work in the detector. It is important to remember that some of these phenomena may only be limited to this sample type, but our limited experimentation suggests rather that they are typical responses. A time constant of 4 seconds is not speedy as far as detectors go, but is sufficiently fast for our purposes in which a typical separation lasts for several minutes at a minimum. Also, in some cases it appears that the detector can operate at higher rates and follow even sharp peaks, though what the difference is is not immediately clear. Clearly the response time for the detector is sufficient for almost any application suggested in this paper to this point.

The strength of the signal above that of the baseline current and above the noise in the system is not constant but depends upon several parameters including voltage, sample size, and flow rate. Figure 7 is several superimposed runs of the detector with identical samples

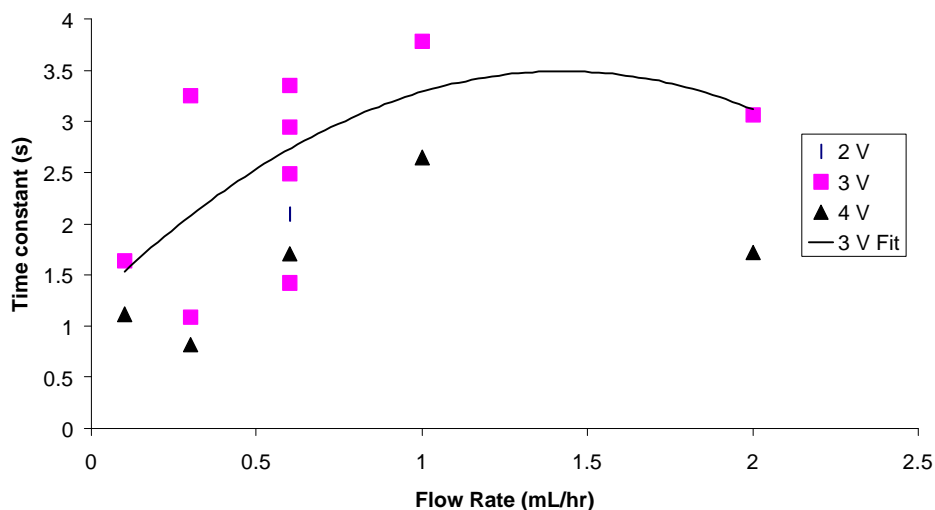


Figure 6. Graph showing time constant to reach steady state for a series of flow rates and voltages.

and flow rates, but varying voltages and corresponding baseline currents. Note that the signal consistently grows with the voltage until the applied potential reaches 8 V. 8 V seems to be the limiting voltage in this case and is the point where electrolysis begins in earnest which can be seen by the failure to reach baseline and then the beginning of exponential current growth after the run (not shown in figure). Note that every other run appears to return to a steady baseline, though the higher the voltage the longer it takes to get to baseline. Note also the consistently low noise whose

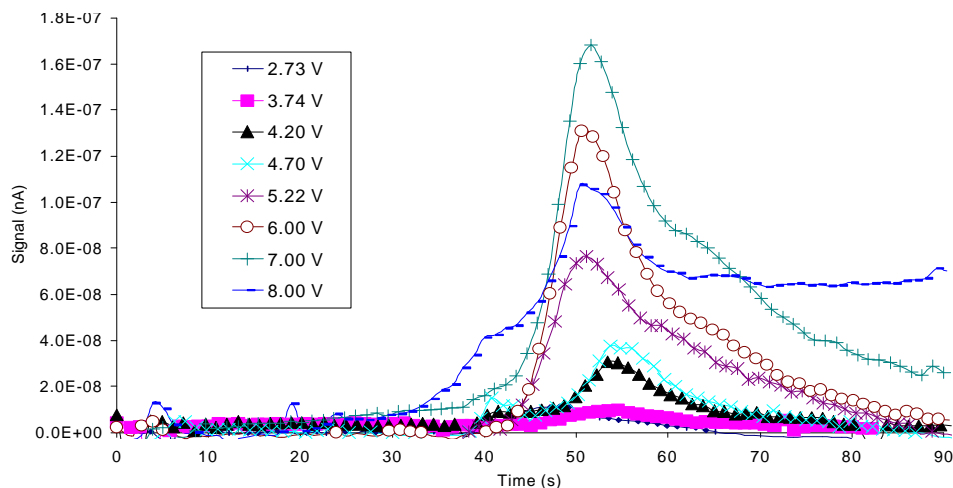


Figure 7. Superimposed acetone samples run through detector at a variety of voltages

absolute magnitude is constant and insensitive to the applied voltage suggesting that the noise is not a function of the applied voltage. As a consequence, the signal-to-noise ratio grows directly with the applied voltage. Figure 8 is a graph showing the maximum signal obtained for a series of tests with only a variation in voltage. The growth in signal and the corresponding signal-to-noise ratio is quite dramatic. The relationship is clearly nonlinear, though there appears to be a range where it may be linear between 4 and 7 V. Notice that at low voltages the signal begins to disappear, though even with applied voltages of 2.5 V, the signal-to-noise ratio is about 20 which is clearly enough for normal operation at high sample concentrations.

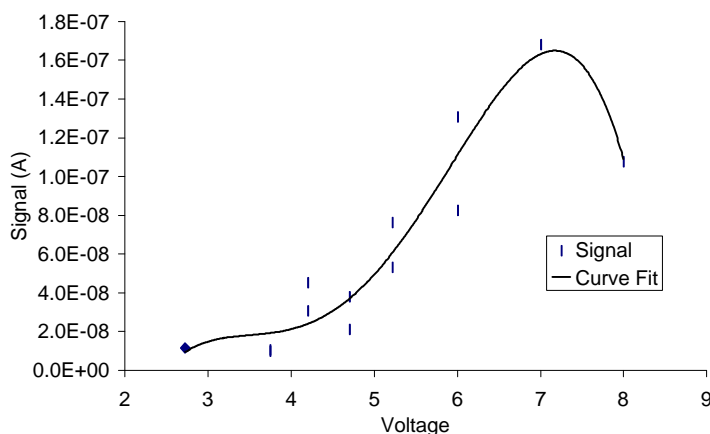


Figure 8. Maximum signal obtained for acetone runs at a series of voltages.

Figure 9 shows superimposed test runs using a decreasing series of acetone concentrations. The data

shows that the percentage of acetone in a constant sample volume does impact the response of the detector and concentration measurements can be made using the detector. Figure 10, though, shows that the relationship is not strictly linear, as expected for a small molecule. Most of this variation takes place at the low concentrations and inspection of the graph seems to indicate that the results may in fact be linear for the higher flow rates with an intercept at 0 as would be expected from the theory described earlier. The nonlinear behavior is almost certainly due to the fact that there is an offset in the signal. Though it is not shown in Figure 10, injections of samples that are identical to the buffer generate a signal slightly smaller than that for 1% acetone. This signal must be

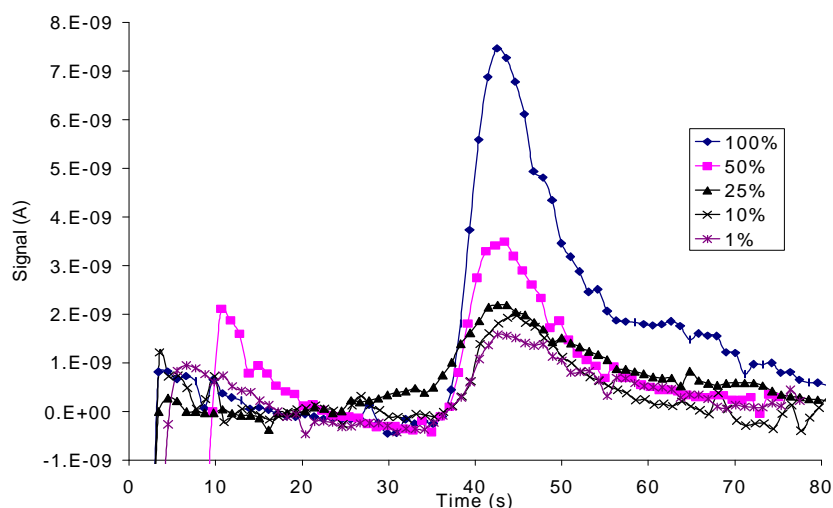


Figure 9. Superimposed acetone samples demonstrating how the concentration of acetone in the sample affects the signal from the detector.

generated by some means not immediately apparent. It is possible that atmospheric gasses such as CO₂ are dissolving in the sample between the time that the buffer is prepared and a sample is injected, or possibly small particles from the syringe or other container are contaminating the solution. Whatever the case, the results show that the detector is capable of detecting very small concentration differences, though if one is not careful an erroneous reading could be generated.

Figure 11 shows several superimposed signals demonstrating how variations in flow rate affect the signal generated. While the function is not as strong as that for the data we looked at previously, a definite pattern still emerges. The signal has a peak at about 1 mL/hr and drops off in both directions from there in a manner similar to that for time constants when compared by flow rate. The effect though is thought to be somewhat different. At high flow rates the residence time for the sample is very short so the net effect of the impedance change is reduced. At low flow

rates, diffusion of the sample away from its center point plays a much greater role and the sample becomes diluted, again reducing the received signal. At a middle point we find the happy medium in which diffusion is minimized but the residence time in the detection area is still significant. Changes in the size of the detection wires may allow for better detection at high flow rates and is currently being studied.

The detector has some limitations that are not immediately apparent upon presentation of this data. While a series of runs closely spaced in time show consistent results, the detector has a tendency to drift over a period of hours which makes for problems with repeatability. The reader may have noticed that for some of the graphs in which a number

of data points were taken for a given input value there is significant scatter. While the signals were clearly discernable, the magnitudes had a tendency to vary from hour to hour and day to day. The equalizing factor seems to be current. In general, the current level seemed to determine the magnitude of the signal more than the applied voltage, though the relationship between current and voltage appeared at times to be somewhat unpredictable. For currents above about 150 nA, though, a good signal was almost always generated with the magnitude proportional to the baseline current.

The drift in the system was somewhat related to voltage as well. At higher voltages, the drift in baseline current was more pronounced. At higher voltages the detector also had a tendency to go unstable after a period of time. For example, at 8 V the detector typically remained stable for only 5 minutes before beginning an exponential climb. At 7 V the detector would

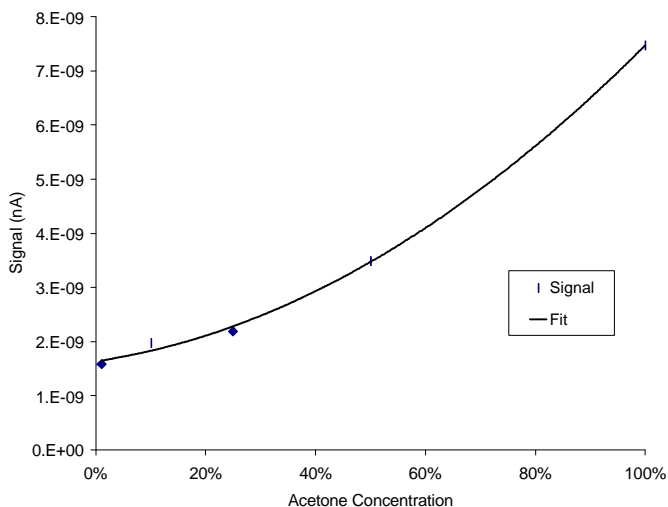


Figure 10. Signal comparison for decreasing acetone concentration showing steady drop in signal for a decrease in acetone concentration.

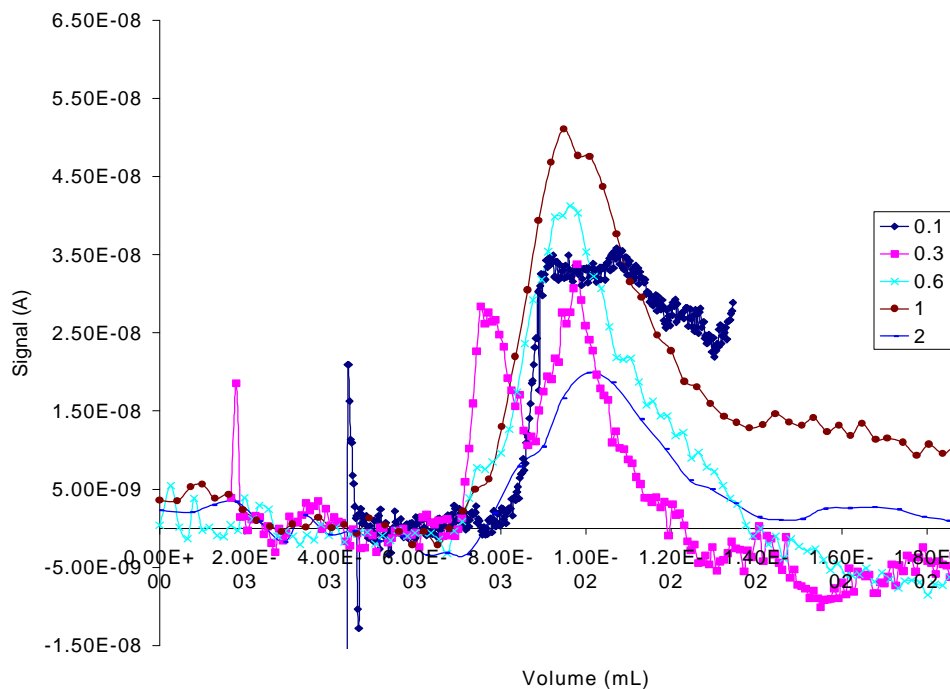


Figure 11. Superimposed acetone runs demonstrating the effect of flow rate on detector response.

last for about 20 minutes for going unstable. The amount of time increased in a similar manner until the detector was operated at about 3.5 V, at which point the system never seems to go unstable. The effect is analogous to that for fatigue in steels in which cycles below a certain force can be performed infinitely many times without failure. This effect may be caused by a material being deposited or removed from one of the electrodes at high voltages, which then allows electrolysis to proceed unhindered.

The noise in the system was generally small relative to the signals measured, but occasionally became quite large for unknown reasons. A voltage shock to the system would generally clear up this difficulty and cause the noise to return to its normal level. Also, on a number of occasions we noticed a sudden shift in baseline without warning and for no apparent reason. Though these shifts were rare enough not to cause great concern, they did cause some loss of data and are worthy of consideration.

With some experience in using the detector, we may now make suppositions as to the mode of operation for the detector with acetone. Acetone is a non-polar molecule and is not anticipated to be highly conductive, yet we see a consistent rise in current when acetone samples pass through the detector. This phenomenon suggests that the major mode of operation is the dispersal of the double layer and the corresponding increase in current. This appears to be the most likely mode for several other non-polar molecules that cause an increase in current as well. On occasion we have seen samples that caused the current to fall from baseline suggesting that all three modes of operation can and do occur in the detector as suggested in the theory section.

Considering all of the data collected so far, we are now in a position to select the optimal operating parameters for the detector to generate the best signal. The time constant data would suggest that a high applied voltage and lower flow rate would be optimal. The voltage data concurs with the higher signal at a higher applied voltage. The signal is maximized for flow rate at about 1 mL/hr, which conflicts somewhat with the time constant data for optimal detection. Considering all of these parameters, we would suggest that the optimal parameters would be with an applied voltage near 4 V, which gives increased signal strength without some of the instability problems of higher voltages. This value improves the time constant relative to lower voltages as well. The flow rate appears optimal at about 0.6 mL/hr. While this value does not generate the lowest time constant or highest signal, it is a middle value that does not exacerbate problems with either of those parameters, but still provides a strong signal. Obviously, the concentration of particles for any sample would be maximized to enjoy the greatest signal-to-noise ratio.

Figure 12 shows the plate height and peak broadening measurements with the off-chip detector. The increasing values for low flow rates indicate that diffusion is beginning to dominate at the low flow rates. Since this effect disappears with the on-chip detector, it is apparent that the diffusion must occur in the detector itself. The reason for the change in the relative importance of diffusion is due to the large dimensions found in the detector compared to the channel itself. Thus in miniaturized separation systems it appears that a requirement of the system will be on-chip detection.

Of particular interest is the difference in band broadening between the system with the on-chip detector and the off-chip detector. The results of band broadening calculations for the systems are shown in Figure 13. The data for the off-chip detector neglects the diffusion-affected data given in Figure 12 for comparison. The band broadening due to the

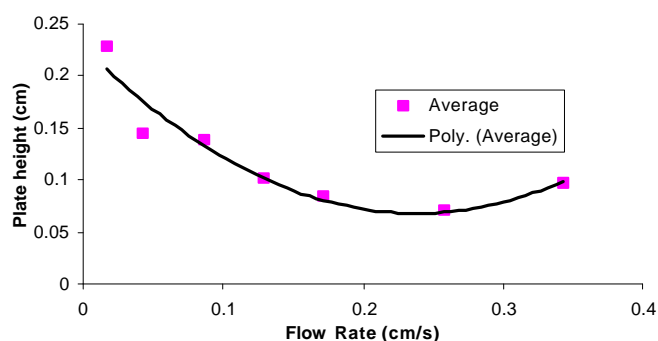


Figure 12. Plate heights for channel using off-chip detector for a series of flow rates.

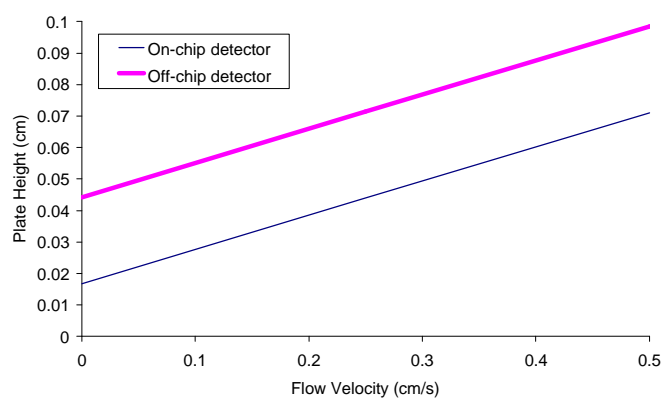


Figure 13. Plate height comparison using on and off chip detection.

instrument itself is indicated by the y-intercept on the graph. Note that band broadening is reduced by more than half when the switch is made to the on-chip impedance detector. The difference in the y-intercept is the measure of improvement.

Once the optimal parameters for detector operation were determined, the detector was used in its intended application with a micromachined electrical field- flow fractionation device. Sample runs are shown in Figure 14 and 15. Figure 14 shows a separation using the off-chip detector and Figure 15 shows a separation using the on-chip conductivity detector. Note the improved separation time for the on-chip detector and the clearly resolved peaks. The resolution for the on-chip detector is at least 50% higher than for the off-chip detector, consistent with the plate height data just presented. While the noise level in Figure 15 is somewhat higher due to the electric field in the channel associated with the operation of the separation system, the peaks for the various particles are clearly distinguished and easily measured. One significant advantage of the detector in these systems is that it quickly goes to baseline when the power is applied- typically in less than ten seconds meaning that the detector could be turned on even after the sample has been injected into the system. Clearly addition of this micromachined conductivity detector to these micro-analysis systems proves a great advantage.

6. CONCLUSIONS

A micromachined impedance detector for particle and chemical detection was designed, fabricated, and characterized. The detector was demonstrated using a number of sample types as well as operation with a micro-analysis system. Some of the advantages of the detector include simplicity of design and operation, fast response and short warm-up time, high signal-to-noise ratio, detection of a wide range of sample types, small size, and compatibility with micromachining processes and VLSI technology for signal processing. While not all facets of the operation of the detector are understood, headway is being made in preparing the device for a wide range of applications. Work is continuing on using both the real and imaginary parts of the impedance to further enhance the signal and improve the operating parameters of the system. Detector dimensions are also being explored to determine if another wire size might be better. Overall, the detector was shown to operate in a consistent manner and to allow detection of a wide range of analytes.

7. ACKNOWLEDGEMENTS

The authors acknowledge support from a National Science Foundation Graduate Research Fellowship, the Whitaker Foundation, Amoco Chemical, and a University of Utah Technology Innovation Grant. The authors would also like to thank Thayne Edwards for his help with data acquisition and the finite element modeling.

8. REFERENCES

1. Z. H. Fan and D. J. Harrison, "Micromachining of capillary electrophoresis injectors and separators on glass chips and evaluation of flow at capillary interconnections," *Anal. Chem.*, vol. 66, p. 177, 1994.

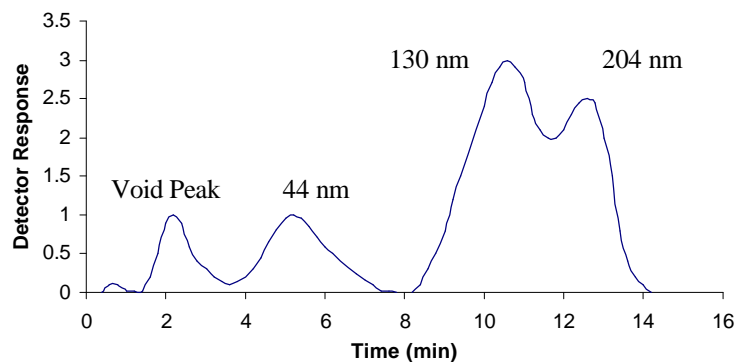


Figure 14. Separation with off-chip detector showing separation of 44, 130, and 204 nm particles. Flow rate was 0.6 mL/hr with a current of 170 μ A.

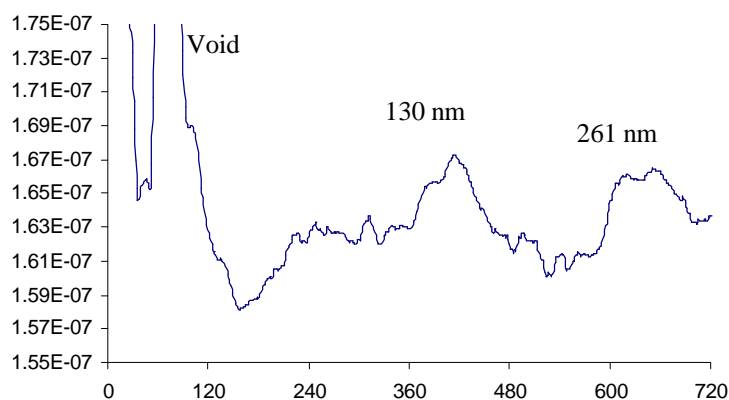


Figure 15. Separation with on-chip detector showing separation of 130 and 261 nm particles. Flow rate was 0.6 mL/hr with a current of 173 μ A.

2. A. Manz, "Miniaturized chemical analysis systems based on electroosmotic flow," in IEEE Micro Electro Mechanical Systems Conf., Nagoya, Japan, Jan. 26-30, 1997.
3. C. S. Effenhauser, A. Manz, and M. H. Widmer, "Glass chips for high-speed capillary electrophoresis separations with submicrometer plate heights," *Anal. Chem.*, vol. 65, pp. 2637-2642, 1993.
4. C. S. Effenhauser, A. Paulus, and A. Manz, "High-speed separation of antisense oligonucleotides on a micromachined capillary electrophoresis device," *Anal. Chem.*, vol. 66, pp. 2949-2953, 1994.
5. S. C. Jacobson, A. W. Moore, and J. M. Ramsey, "Fused quartz substrates for microchip electrophoresis," *Anal. Chem.*, vol. 67, pp. 2059-2063, 1995.
6. A. T. Woolley, and R. A. Mathies, "Ultra-high-speed DNA sequencing using capillary electrophoresis chips," *Anal. Chem.*, vol. 67, pp. 3676-3680, 1995.
7. H. Nakanishi, T. Nishimoto, N. Nakamura, S. Nagamachi, A. Arai, Y. Iwata, and Y. Mito, "Fabrication of electrophoresis devices on a quartz and glass substrates using a bonding with HF solution," in IEEE Micro Electro Mechanical Systems Conf., Nagoya, Japan, Jan. 26-30, 1997.
8. N. Chiem and D.J. Harrison, "Microchip-based Capillary Electrophoresis for Immunoassays: Analysis of Monoclonal Antibodies and Theophylline," *Anal. Chem.*, vol. 69, pp. 373-378, February 1, 1997.
9. D. E. Raymond, A. Manz, and H. M. Widmer, "Continuous sample pretreatment using a free-flow electrophoresis device integrated onto a silicon chip," *Anal. Chem.*, vol. 66, pp. 2858-2865, 1994.
10. D. E. Raymond, A. Manz, and H. M. Widmer, "Continuous separation of high molecular weight compounds using a microliter volume free-flow electrophoresis microstructure," *Anal. Chem.*, vol. 68, pp. 2515-2522, 1996.
11. B. K. Gale, A. B. Frazier, and K. Caldwell, "Micromachined electrical field-flow fractionation (μ -EFFF) system," in IEEE Micro Electro Mechanical Systems Conf., Nagoya, Japan, Jan. 26-30, 1997.
12. B. K. Gale, K. D. Caldwell, and A. B. Frazier, "A Micromachined Electrical Field- Flow Fractionation System" *IEEE-TBE*, in press.
13. M. A. Northrup, C. Gonzalez, D. Hadley, R. F. Hills, P. Landre, S. Lehew, R. Saiki, J. J. Sninsky, and R. Watson, "A MEMS-based miniature DNA analysis system," in Proc. Transducers 95, Stockholm, Sweden, June 25-29, 1995.
14. P. Wilding, M. A. Shoffner, and L. J. Kircka, "Manipulation and flow of biological fluids in straight channels micromachined in silicon," *Clin. Chem*, vol. 40, p. 1815, 1994.
15. M. Albin, R. Kowallis, E. Picozza, Y. Raysberg, C. Sloan, E. Winn-Deen, T. Woudenberg, and J. Zupfer, "Micromachining and microgenetics, what are they and where do they work together?" in IEEE Solid-State Sensor and Actuator Workshop, Hilton Head, SC, June 2-6, 1996.
16. R. C. Anderson, G. J. Bogdan, and R. J. Lipshutz, "Miniaturized genetic-analysis system," in IEEE Solid-State Sensor and Actuator Workshop, Hilton Head, SC, June 2-6, 1996.
- 17-. S. C. Terry, J. H. Jerman, and J. B. Angell, "Gas-chromatographic air analyser fabricated on silicon wafer," *IEEE Trans. Electron. Devices*, vol. 26, pp. 1880-1886, 1979.
18. R. R. Reston and E. S. Kolesar, "Silicon-micromachined gas chromatography system used to separate and detect ammonia and nitrogen dioxide--part I: design, fabrication, and integration of the gas chromatography system," *IEEE J. Microelectromech. Sys.*, vol. 3, p. 134, 1994.
19. R. R. Reston and E. S. Kolesar, "Silicon-micromachined gas chromatography system used to separate and detect ammonia and nitrogen dioxide--part II: evaluation, analysis, and theoretical modeling of the gas chromatograph system," *J. Microelectromech. Sys.*, vol. 3, p. 147, 1994.
20. S. J. Doherty, and W. L. Winniford, "Rapid on-line analysis using a micromachined gas chromatograph coupled to a bench-top quadrupole mass spectrometer," *LC-GC*, vol. 12, pp. 846-850, 1994.
21. R. A. Mowery, "Determining the calorific value of natural gas using a silicon micromachined process gas chromatographic analyzer," *ISA Transactions*, vol. 25, pp. 1-9, 1986.

22. G. Ocvirk, E. Verpoorte, A. Manz, H. M. Widmer, "Integration of a micro liquid chromatograph on to a silicon chip," in *Proc. Transducers '95*, 1995, p. 191.
23. A. Manz, Y. Miyahara, J. Miura, Y. Watanabe, H. Miyagi, and K. Sato, *Sensors & Actuators*, vol. B1, p. 249, 1990.
24. P. Wilding, M. A. Shoffner, and L. J. Kircka, "Manipulation and flow of biological fluids in straight channels micromachined in silicon," *Clin. Chem.*, vol. 40, p. 1815, 1994.
25. A. W. Moore, S. C. Jacobson, and J. M. Ramsey, "Microchip separations of neutral species via micellar electrokinetic capillary chromatography," *Anal. Chem.*, vol. 67, pp. 4184-4189, 1995.
26. B. K. Gale, K. D. Caldwell, and A. B. Frazier, "Characterization of a Micromachined Electrical Field- Flow Fractionation System" in *Proc. Solid-State Sensor and Actuator Workshop*, Hilton Head, SC, June 8-11, 1998, pp. 342-345.
27. H. Ayliffe, R. Rabbitt, P. Tresco, and B. Frazier, "micromachined Cellular Characterization System for Studying the Biomechanics of Individual Cells," in *Proc. Transducers '97*, Chicago, IL, June 16-19, pp. 1311-1314.
28. M. A. Brett and A. M. O. Brett, *Electrochemistry: Principles, Methods, and Applications*. Oxford: Oxford Univ. Press, 1993.
29. K. D. Caldwell and Y. S. Gao, "Electrical field-flow fractionation in particle separation. Monodisperse standards," *Anal. Chem.*, vol. 65, pp. 1764-1772, July 1, 1993.
30. A.S. Said, *Theory and Mathematics of Chromatography*. Heidelberg, Germany: Dr. Alfred Huethig Publishers, 1981.